Horizontal and Vertical Structure of Easterly Waves in the Pacific ITCZ

Yolande L. Serra[1], George N. Kiladis[2], and Meghan F. Cronin[3]

[1] Department of Atmospheric Sciences, University of Arizona, Tucson AZ
[2] NOAA Physical Sciences Division, ESRL, Boulder, CO
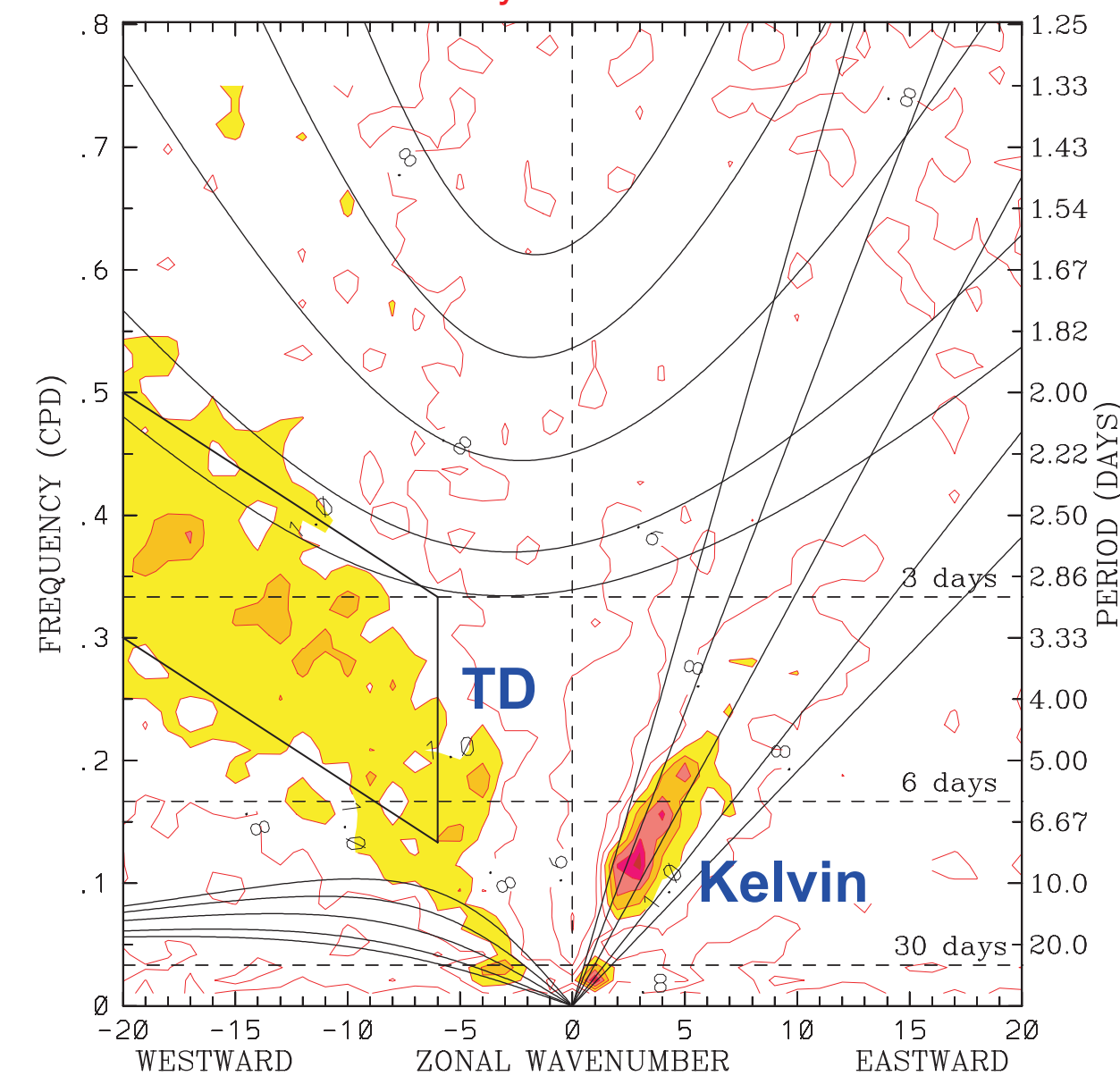[3] NOAA Pacific Marine Environmental Laboratory, Seattle, WA

1 Introduction and Methodology

This poster highlights a portion of the results of a project entitled "Investigation of Synoptic Disturbances and their Effect on the Boundary Layer and SST in the East Pacific ITCZ on Seasonal and Interannual Time Scales", funded by the Climate Prediction Program for the Americas of NOAA's Climate Program Office.
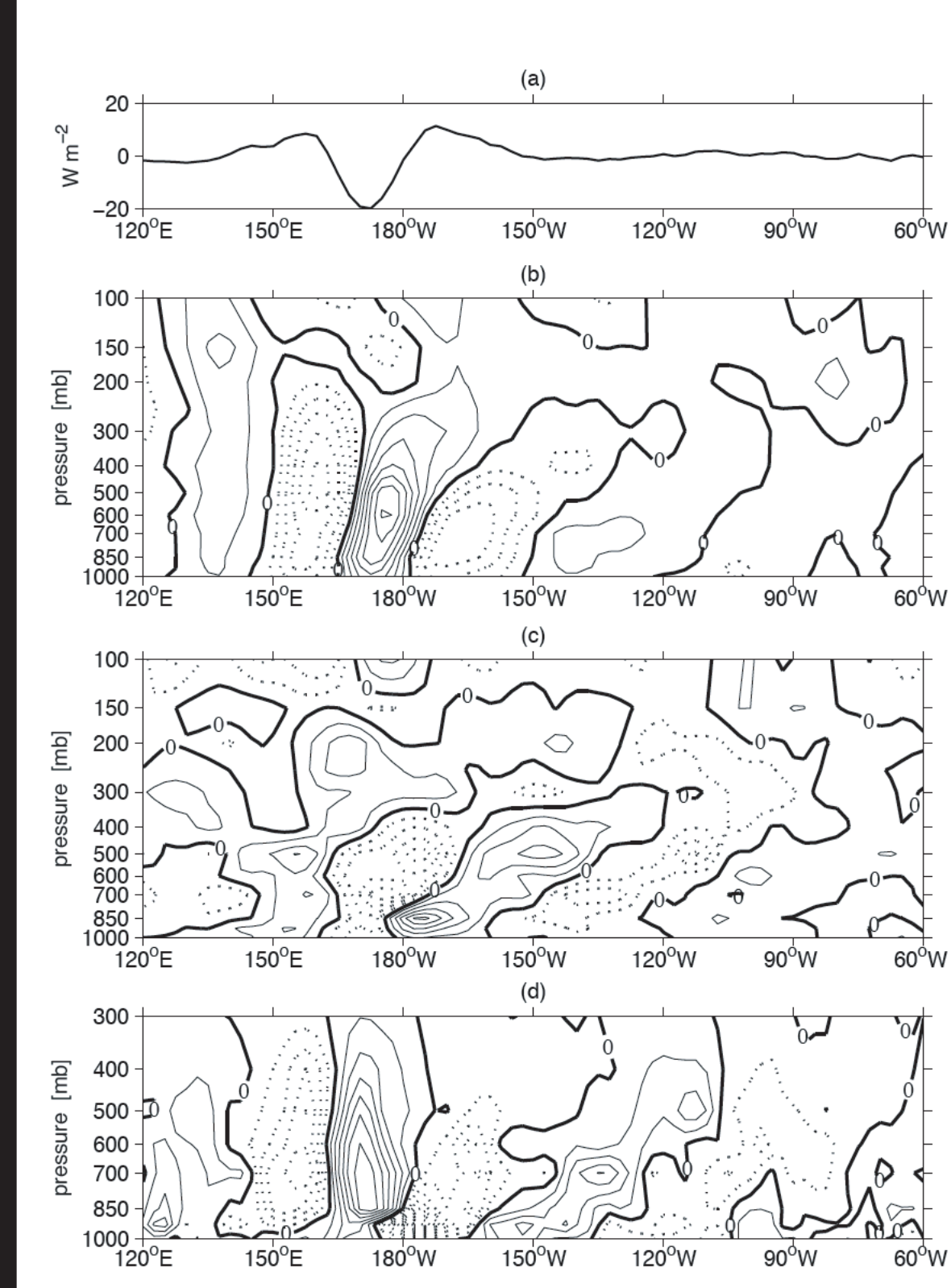
This phase of the project analyzes the structure of easterly waves using TAO buoy, radiosonde, satellite-derived Outgoing Longwave Radiation (OLR) and the NCEP/NCAR reanalysis data sets (Serra et al. 2006).

Easterly waves are isolated through space-time filtering of OLR using the methodology of Wheeler and Kiladis (1999). Below is a space-time spectrum of OLR for June-November 1979-2003, the period of study. A spectral peak associated with Kelvin waves show up clearly, as does the so-called "TD-band" of westward moving waves in the wavenumber 5-20 range. Kiladis et al. (2006) show that an inverse transform of TD-band filtered OLR can be used as an index for African easterly waves, as is done here for the Pacific disturbances.

Dynamical fields from TAO, reanalysis and radiosonde data are regressed onto TD-filtered OLR at various grid point to isolate the structural differences of easterly waves across the Pacific ITCZ.

2 Surface Variability

TAO/TRITON and TAO/EPIC buoys and CARDS stations used for this study overlaid on OLR for June-November 1979-2002.

Power spectral density of (a) meridional wind, (b) zonal wind, (c) air temperature, and (d) specific humidity shown in variance preserving format using data from all TAO/TRITON buoys along 5°N and 8°N in the Pacific. Gray vertical lines indicate 3- and 6-day periods. Dashed lines are 95% confidence limits. Values of the temperature peaks at the diurnal and semi-diurnal periods are indicated above the black triangles in (c).
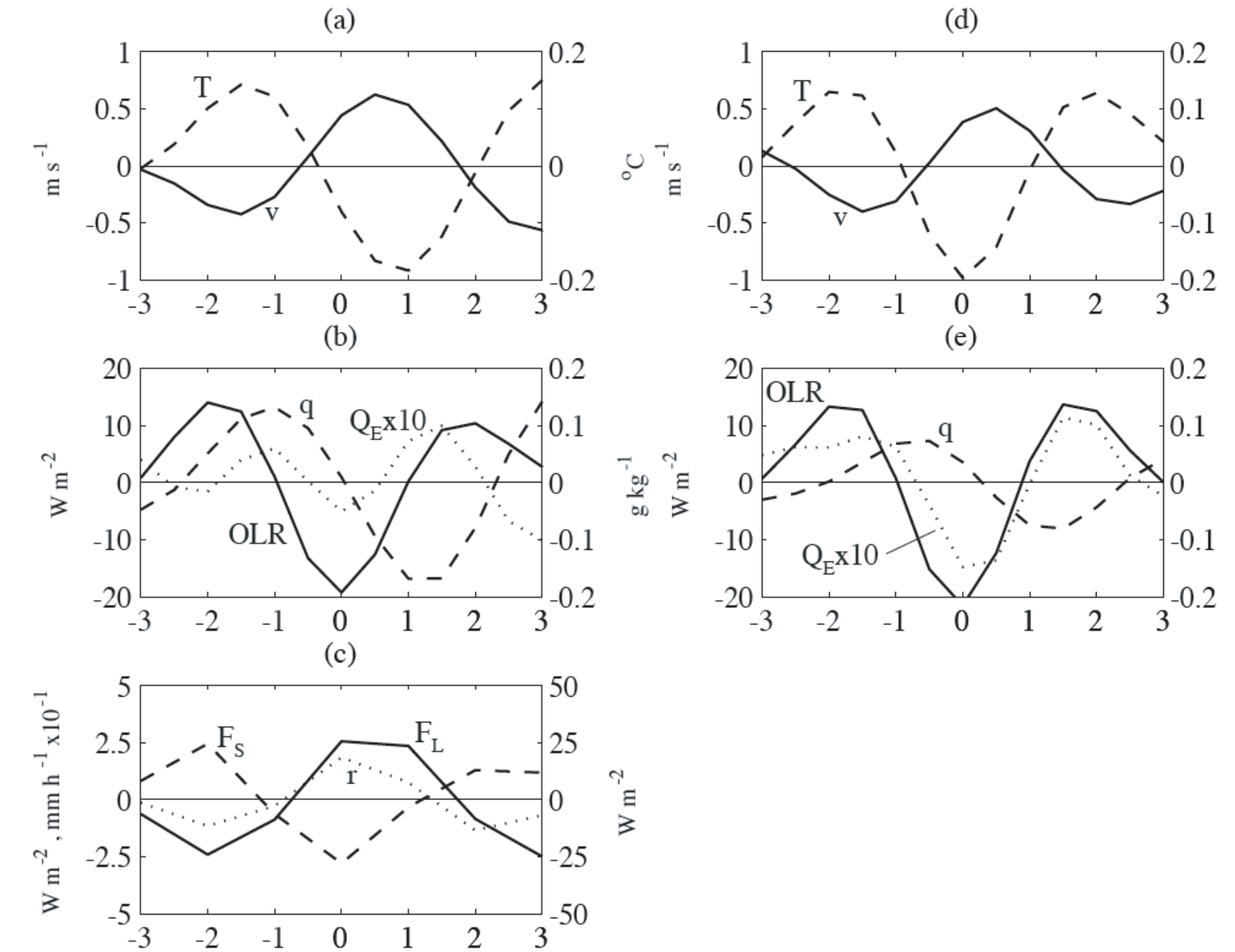
Regressions of buoy (a) meridional wind (solid: v) and air temperature (dashed: T); (b) specific humidity (dashed: q) and latent heat flux (dotted: QE); and (c) longwave cloud forcing (left axis: solid: FL), shortwave cloud forcing (right axis: dashed: FS) and rain rate (dotted: r) all at 10°N 95°W. Also shown in (b) is TD-filtered OLR at 10°N 95°W (solid: OLR). (d)-(e) same as (a)-(b) but for buoy at 8°N 165°E using an OLR base point at 7.5°N 165°E. QE has been multiplied by 10 to match range of OLR values.

On the left variance-conserving power spectra are averaged from 1990-2003 over all available TAO moorings at 5N and 8N. 3-6 day variability is predominant in the zonal and meridional wind, surface air temperature, and specific humidity in all of these plots, along with the diurnal and semidiurnal cycles. Much of the 3-6 day synoptic variability can be attributed to easterly waves, as well as mixed Rossby-gravity waves

The regressions above show that anomalously warm and humid conditions within northerlies lead TD-filtered OLR by a day or so at the buoys considered. Maximum cloudiness and rainfall and a minimum in latent heat flux is associated with the OLR minimum, within anomalous southerly flow at these locations. A reduction of shortwave but an enhancement of longwave radiation also accompanies the rainfall and continues for a couple of days afterwards. The latter signal is consistent with Petersen et al.'s (2003) observations during the passage of easterly waves during the EPIC field campaign.

3 Horizontal Structure
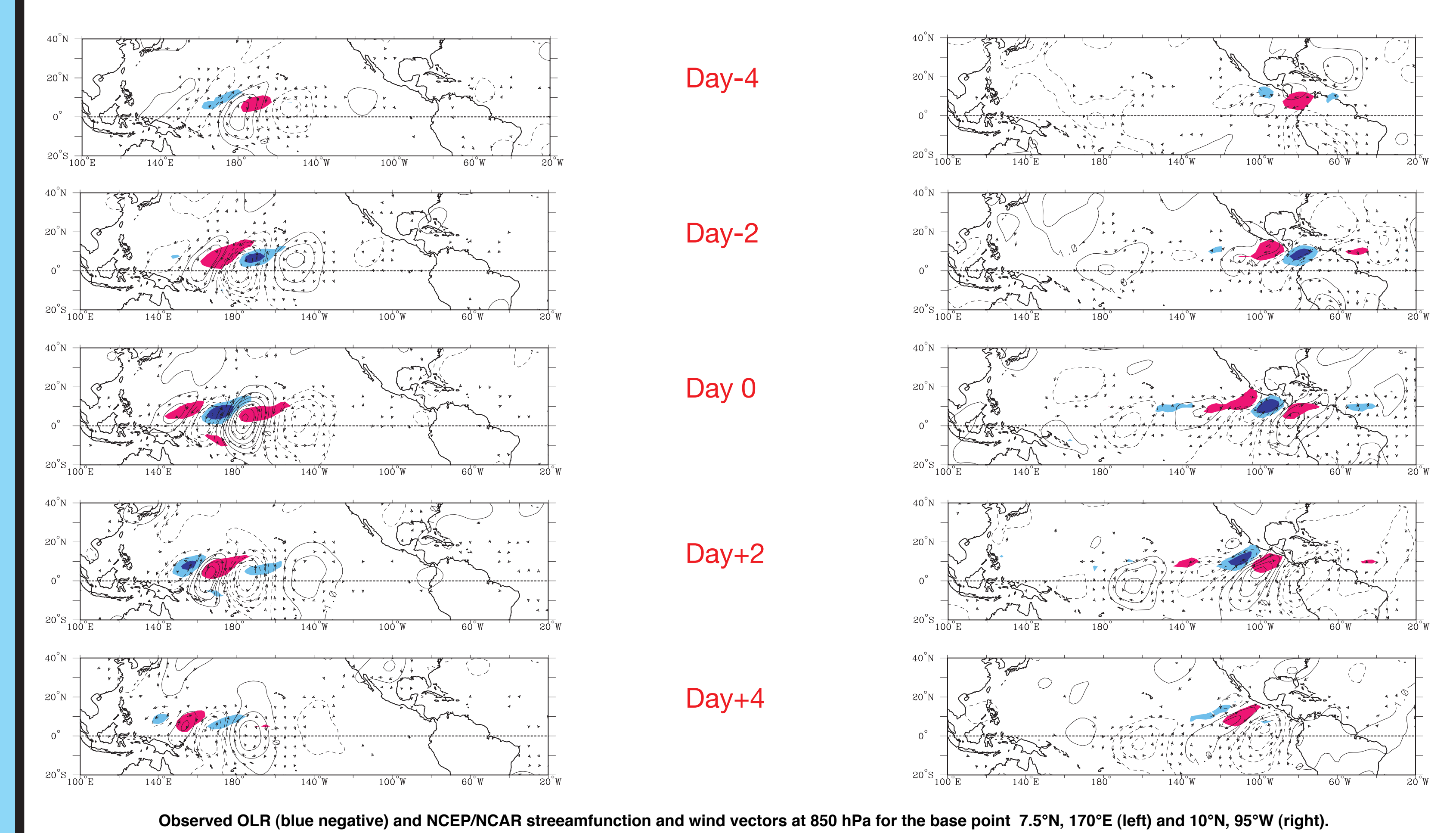
Observed OLR (blue negative) and NCEP/NCAR streamfunction and wind vectors at 850 hPa for the base point 7.5°N, 170°E (left) and 10°N, 95°W (right).

In the left plot OLR and the flow at 850 hPa are regressed against TD-filtered OLR at the point 7.5°N, 170°E at various lags. Anomalous eddies are centered just north of the equator, which when added to the mean flow yield the characteristic "inverted trough" signature of easterly waves (e.g. Serra and Houze 2002). Convection (blue region) occurs in southerly flow as the wave crosses the basin, then shifts into the trough over the western Pacific. At later lags the circulations then move off the equator towards the northwest (not shown). The circulation signal extends well to the south of the equator.

A plot for the base region 10°N, 95°W is shown on the right. Convection occurs to the northeast of the strongest cyclonic circulation in southwesterly flow. The eddies are much more positively tilted than those farther west, implying stronger barotropic energy conversion of zonal kinetic to eddy kinetic energy, with a flux of easterly momentum away from an easterly jet maximum at around 15°N. This conversion is likely not sufficient to initiate these waves but may help rejuvenate them, given a substantial signal of convection and circulation over the Atlantic preceding their amplification off the coast of Central America.
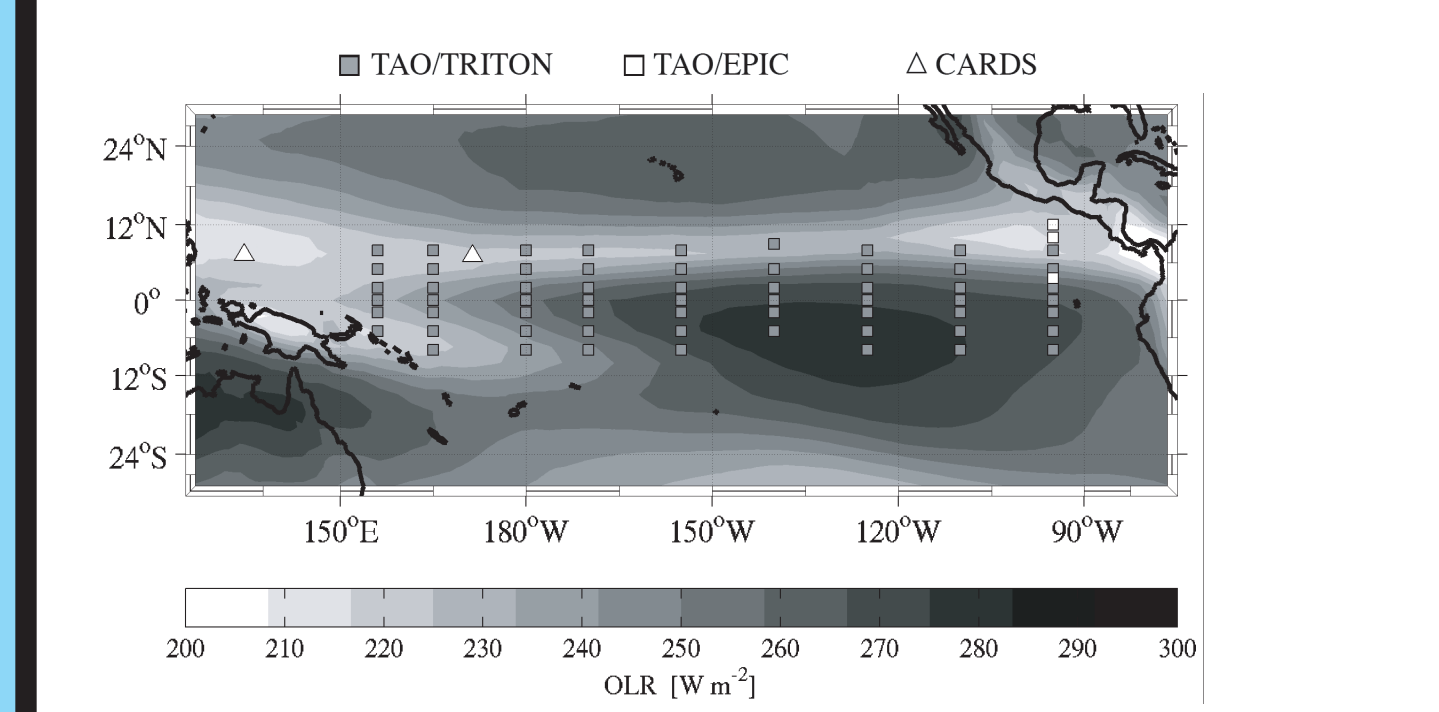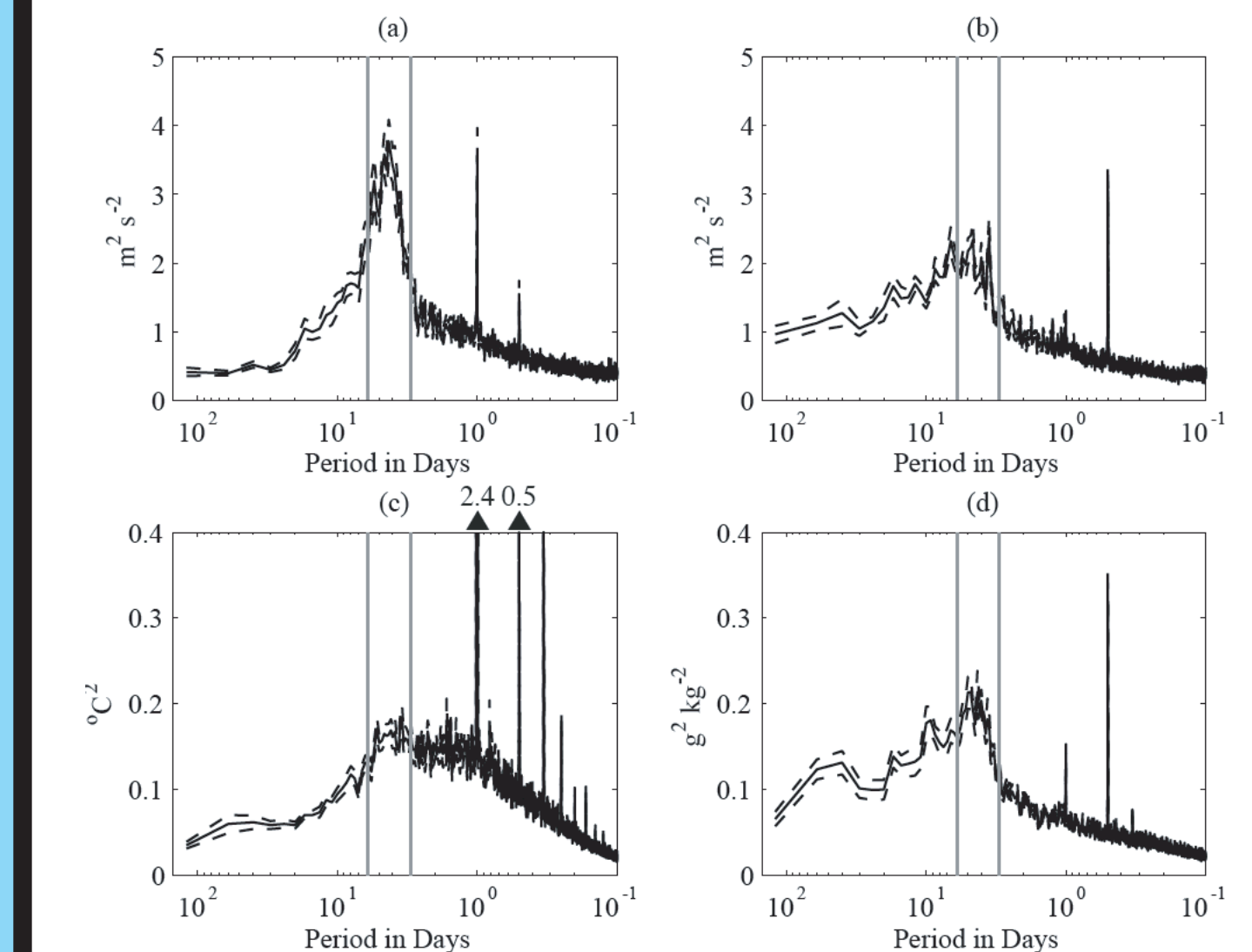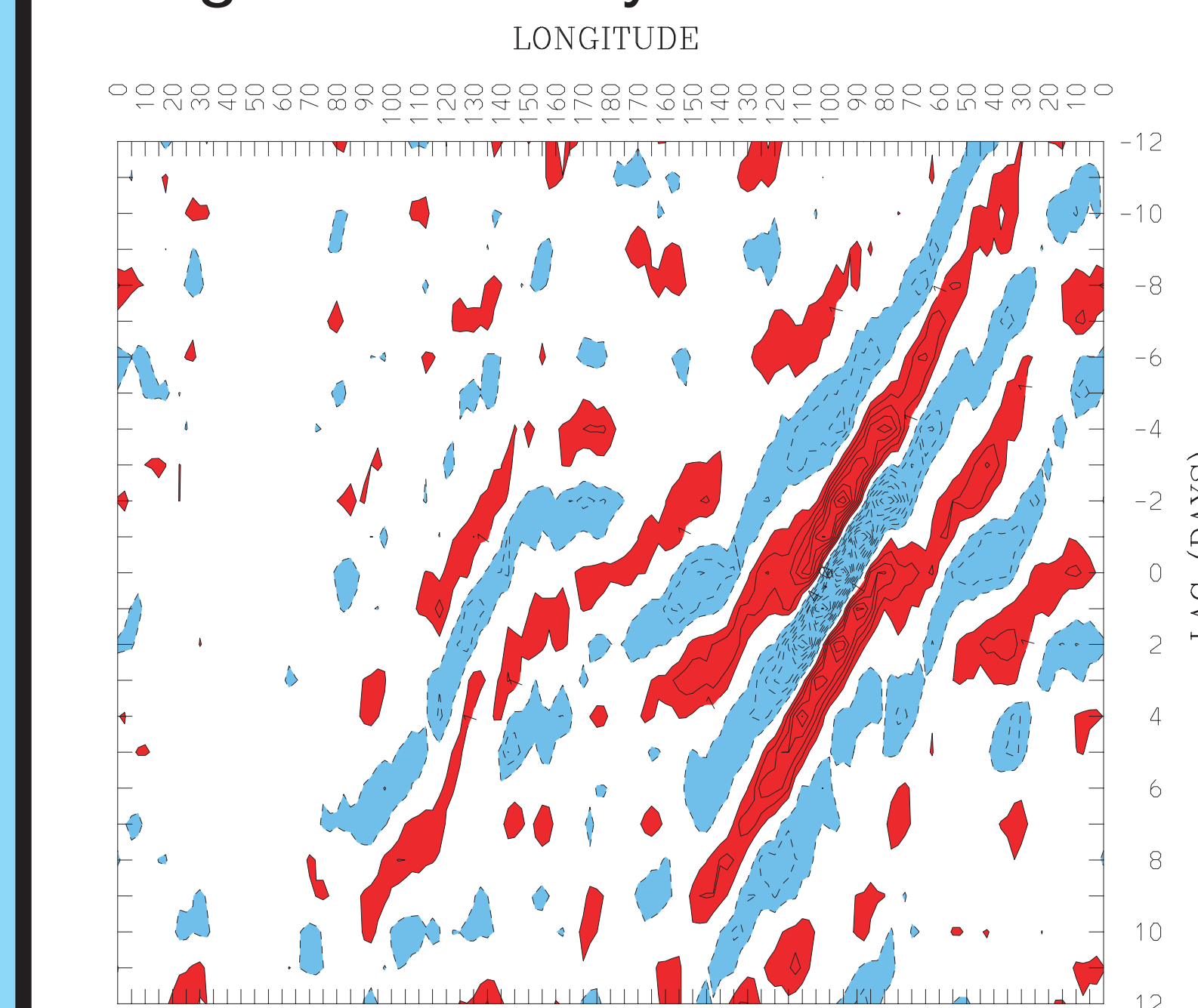
4 Vertical Structure

Profiles along 7.5°N of (a) TD-filtered OLR and NCEP/NCAR (b) meridional wind, (c) air temperature, and (d) specific humidity regressions for base point at 7.5°N 170°E). Positive anomalies are shown as solid contours and negative anomalies are shown as dotted contours. Contour intervals are 0.15 m s-1, 0.02 °C, and 0.02 g kg-1.

(a) TD-filtered OLR and profiles of (b) meridional wind (c) air temperature, and (d) specific humidity regressions at Majuro (7.1°N 171.4°E). (e)-(h) same as (a)-(d) but for Koror (7.3°N 134.5°E). Positive anomalies are shown as dark shading and negative anomalies are shown as light shading. Contour intervals are 0.1 m s-1, 0.1 °C, and 0.1 g kg-1.

Above are plots of the vertical structure of meridional wind, air temperature, and specific humidity from reanalysis (left), and radiosonde at Majuro (middle) and Koror (right). Reanalysis shows strongly upward and eastward tilted structures over the eastern Pacific, which become more upright as the waves propagate to the west. This is confirmed by the radiosondes, with Koror structures almost vertically oriented or even tilting westward with height, as in the meridional wind. In all cases anomalous warmth and moistening occurs first at the surface ahead of the waves, with rapid moistening of the entire column during deepest convection, followed by cooling and drying first at the surface while it remains moist aloft. This suggests a transition from shallow to deep convection, then to stratiform precipitation as the wave passes by. The temperature signal is for the most part consistent with waves over Africa (Kiladis et al. 2006), with a complex higher mode vertical structure, and with early work on the vertical structure of Pacific easterly waves (Reed and Recker 1971).

5 Origin of Easterly Waves

Hovmoller of OLR regressions at 10°N for the base point at 10°N 95°W. Dark gray contours are negative anomalies, lighter gray contours are positive anomalies. Contour lines are draw at intervals of 2 W m-2 starting at ±1 W m-2.

This Hovmoller diagram shows the regressed OLR for the eastern Pacific point along 10°N, over a global domain. OLR perturbations clearly start over the Africa in this picture, and propagate westward at about 10 m s-1, with a wavelength of around 3850 km. In this picture the convective signal disappears near the dateline. The diagram also shows that easterly waves tend to appear as a "wavepacket" of several periodic disturbances.

Similar diagrams for points farther west over the central and western Pacific (not shown) reveal that for waves west of around 120°W, the convective signals originate to the west of Central America, as do the associated dynamical signals in vorticity or meridional wind.

From this we can conclude that most of the easterly waves that affect the Pacific originate within that basin, but evidently some of the waves over the Atlantic can cross the American land mass and strengthen once they reach the Pacific.

6 Energetics
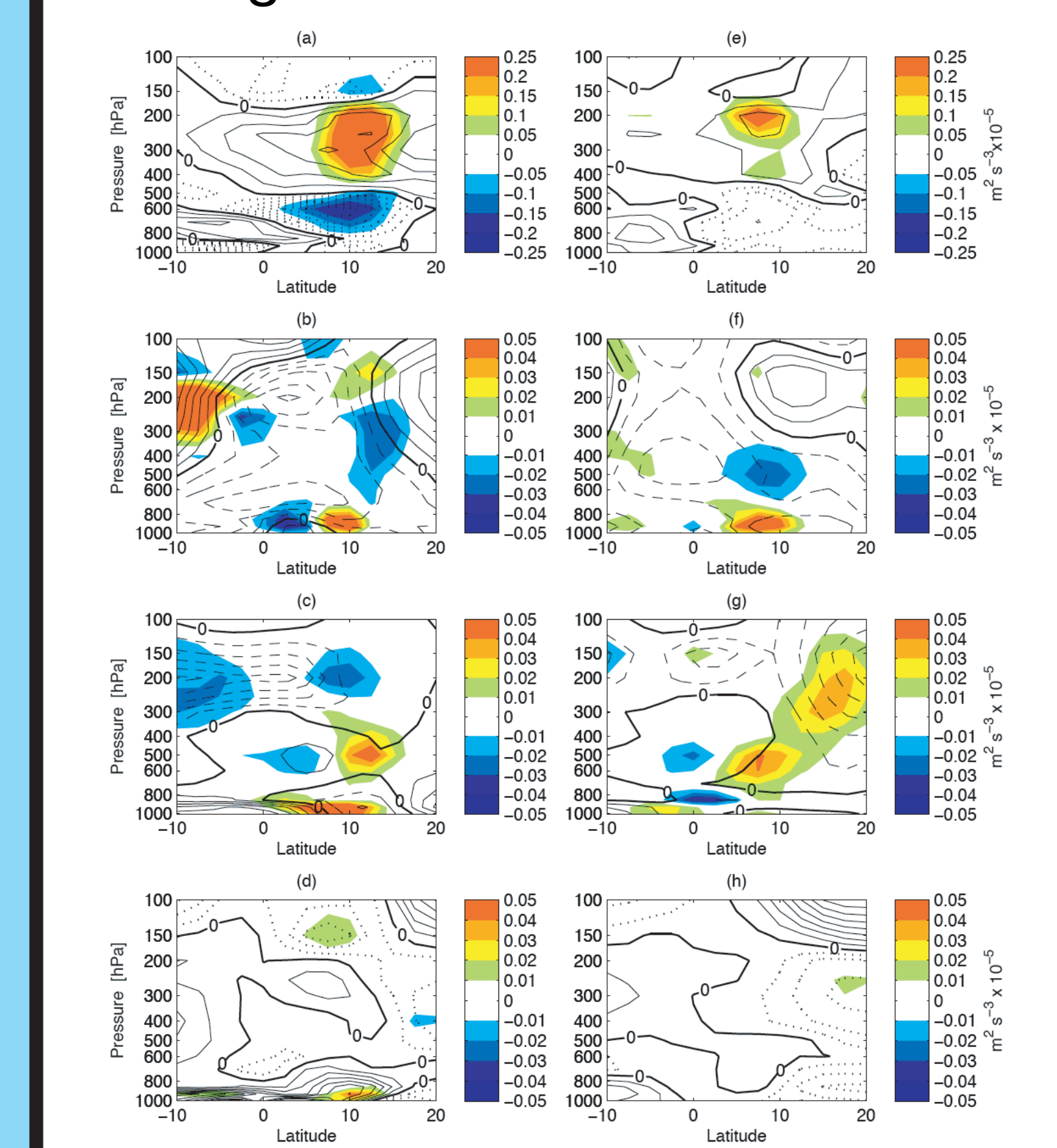
Meridional sections of (a) T' and CAE→KE, (b) uclim and CKU→KE term 1, (c) vclim and CKU→KE term 2, and (d) dTclim/dy and CAU→KE term 1 for base point at 10°N 95°W. Contour intervals are 0.02°C, 2 m s-1, 1 m s-1, and 0.05°C km-1 for (a)-(d), respectively. (e)-(h) same as (a)-(d) but for base point at 7.5°N 170°W.

Energy conversion terms are calculated as in Norquist et al. (1977) using Jun.-Nov. climatological values for the means and regressed quantities as perturbation terms, averaging over Day-4 through Day+4. The dominant energy source for both locations is the conversion of available to kinetic energy (CAE to KE in a and e above), implying that convectively driven motions are crucial to the maintenance of Pacific easterly waves. This is in contrast to waves over Africa, where barotropic conversion from the mean jet flow is dominant (CKU to KE in b and f). In Pacific waves, these terms are small and have a complex structure.

7 Conclusions

* Easterly wave structure varies systematically over the Pacific, with convection occuring in low level southwesterly flow over the east, more southerly flow over the central, and in the trough or slightly into northerly flow over the westernmost Pacific.

* The vertical structure of the flow in easterly waves also varies across the Pacific, having eastward tilts with height over the east, and progressively more upright then westward tilts towards the west.

* A warm, moist boundary layer is observed ahead of the waves, with moisture being quickly lofted through the troposphere by deep convection, followed by a signal of drying and cooling after the passage of the wave. This is consistent with a progression from shallow to deep convection, followed by stratiform precipitation as the wave passes.

* Energetics calculations imply that Pacific easterly waves are driven primarily by convective motions, with relatively weak adiabatic barotropic and baroclinic conversion terms. This differs from African easterly waves, where the latter appear to be dominant.

* Most of the easterly waves affecting the Pacific appear to originate within that basin, although at least some of the waves over the eastern Pacific have their origins over the Atlantic, crossing Central America.

* Ongoing work is examining details of the surface energy budget of easterly waves, and the ability of regional models to capture the waves.

References:

Kiladis, G.N., C. D. Thorncroft, and N. M. J. Hall, 2006: Three dimensional structure and dynamics of African easterly waves. Part I: Observations. J. Atmos. Sci., 63, (in press).

Norquist, D.C., E.E. Recker, and R.J. Reed, 1977: The energetics of African wave disturbances as observed during Phase III of GATE. Mon. Wea. Rev., 105, 334-342.

Petersen, W.A., R. Cifelli, D. J. Boccippio, S. A. Rutledge, and C. Fairall, 2003: Convection and easterly wave structures observed in the eastern Pacific warm pool during EPIC 2001. J. Atmos. Sci. 60, 1754-1773.

Reed, R. J. and E. E. Recker, 1971: Structure and properties of synoptic-scale wave disturbances in teh equatorial western Pacific. J. Atmos. Sci. 28, 1117-1133.

Serra, Y. L., and R. A. Houze, 2002: Observations of variability on synoptic time scales in the east Pacific ITCZ. J. Atmos. Sci., 59, 1723-1743.

Serra, Y. L., G. N. Kiladis, and M. F. Cronin, 2006: Horizontal and vertical structure of easterly waves in the Pacific ITCZ. J. Climate, (in revision).

Wheeler, M., and G. N. Kiladis, 1999: Convectively coupled equatorial waves: Analysis of clouds and temperature in the wavenumber-frequency space. J. Atmos. Sci., 56, 374-399.